

SETTING UP TRAFFIC LIGHT SYSTEM THRESHOLDS FOR GEOTHERMAL STIMULATION IN HELSINKI, FINLAND

Thomas ADER¹, Michael CHENDORAIN², Matthew FREE³, Tero SAARNO⁴,
Pekka HEIKKINEN⁵, Peter Eric MALIN⁶, Peter LEARY⁷, Grzegorz KWIA TEK⁸,
Georg DRESEN⁹, Felix BLÜMLE¹⁰, Tommi VUORINEN¹¹

Abstract: *St1 Deep Heat is developing a geothermal doublet for the purpose of delivering deep geothermal heat to local district heat networks. As part of the project, a first well was drilled to a vertical depth of 6.1 km near Helsinki, Finland, and was stimulated in June-July 2018 in order to improve rock permeability. Given that the stimulation took place in a densely populated area with multiple sensitive receptors, a seismic Traffic Light System (TLS) was required before the start of well stimulation activities. The TLS thresholds were established in a probabilistic way, in order to account for uncertainties in the data available. The thresholds were based on a combination of the surface expression of induced seismicity and associated magnitudes, so that false alarms related to surface expression not due to an induced seismic event could be avoided. For the 2018 stimulation, peak ground velocity (PGV) of 1 mm/s associated with a $M_L \geq 1$ event triggered an Amber alert, while a PGV of 7.5 mm/s associated with a $M_L \geq 2.1$ event triggered a Red alert. Specific thresholds based on PGV and peak ground acceleration (PGA) were gathered for sensitive receptors and related to earthquake magnitudes.*

Introduction

The St1 Deep Heat (St1 DH) project is developing a geothermal doublet for the purpose of delivering deep geothermal heat to local district heat networks. As part of the project, a 6.1 km deep well, OTN-3, was drilled as a geothermal injector. This well was drilled to the stimulation depth of 6.1 km, completed in May 2018. OTN-3 was then stimulated for seven weeks, starting in June 2018, in order to improve the rock permeability in contact with the well (Kwiatek et al., 2019).

The project is located in the Otaniemi neighbourhood in the City of Espoo, which is located just west of Helsinki in Finland (Figure 1).

The City of Espoo's buildings department required that a seismic 'Traffic Light System' (TLS) be developed and approved before granting permission for St1 DH to perform well stimulation activities. The Institute of Seismology at the University of Helsinki (ISUH) was appointed by the City of Espoo to provide consultation on the St1 DH proposed TLS and associated monitoring network.

¹ Senior Consultant, Arup, London, UK, thomas.ader@arup.com

² Associate, Arup, London, UK

³ Director, Arup, London, UK

⁴ Project Director, St1 Deep Heat Oy, Helsinki, Finland

⁵ Scientific Advisor, St1 Deep Heat Oy, Helsinki, Finland

⁶ Research Professor, GFZ, Potsdam, Germany

⁷ Researcher, Advanced Seismic Instrumentation & Research, Dallas, TX, USA

⁸ Senior Researcher, GFZ, Potsdam & Free University, Berlin, Germany

⁹ Professor, GFZ, Potsdam, Germany

¹⁰ Geophysicist, fastloc GmbH, Berlin, Germany

¹¹ Seismologist, Institute of Seismology, University of Helsinki, Finland

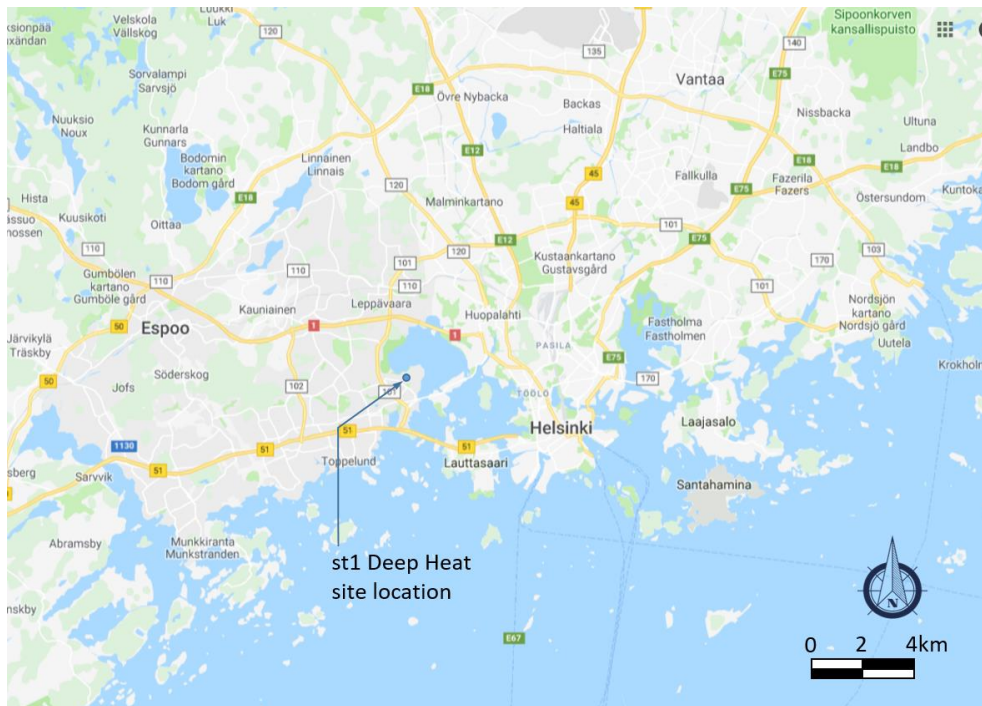


Figure 1: St1 Deep Heat Site Location

TLS Monitoring Networks

An effective TLS relies on a real-time seismic monitoring system and leverages this information to mitigate the risk of negative public response and the risk to the built environment.

The TLS for the stimulation in Finland relied on the input of two seismic monitoring networks (Figure 2): a 12-station borehole network composed of seismometers installed in boreholes between 300 m and 1,150 m depth (the Satellite Network) and a 14-station surface network composed of geophones placed at strategic surface locations, such as nearby critical infrastructure sites (the Surface Network).

An observation well, OTN-2, was drilled a few meters away from OTN-3 to a depth of 3.3 km and instrumented with a 12-level string of 3-component seismometers, at depths from 2,200 m to 2,630 m. The satellite network and this vertical array were used to locate the source of seismic events and estimate their other source parameters, such as time and magnitude. The surface network measured the amplitude of the surface expression of seismic events. The installation and maintenance of the satellite network was performed by *Advanced Seismic Instrumentation & Research (ASIR)*, while the localization of the seismic events and computation of source parameters in near-real time was undertaken by *fastloc GmbH*. The surface network was installed and maintained by the local company *Kalliotekniikka Consulting Engineers Oy*.

The exact azimuthal gap of the networks depended on the location of the seismic event, but for events located at the drilling site, the maximum azimuthal gaps were about 65° for the surface network and 70° for the satellite network. Note that the surface network was not used for earthquake localisation, so that its azimuthal gaps were of little importance for the implementation of the TLS.

As a requirement of the TLS plan, all stations used for monitoring TLS conditions had to be operational for a period of at least one month prior to stimulation. During the stimulation of OTN-3, the maximum allowed number of satellite station outages was when the azimuthal gap at the centre of the satellite network remained less than 130° and when more than five satellite stations were operating.

The seismic observations made during the stimulation have been reported by Kwiatek *et al.* (2019, in press). Using the TLS guidelines and near-real time calculation of induced earthquake source parameters, a seismicity-controlled stimulation feedback loop was instituted.

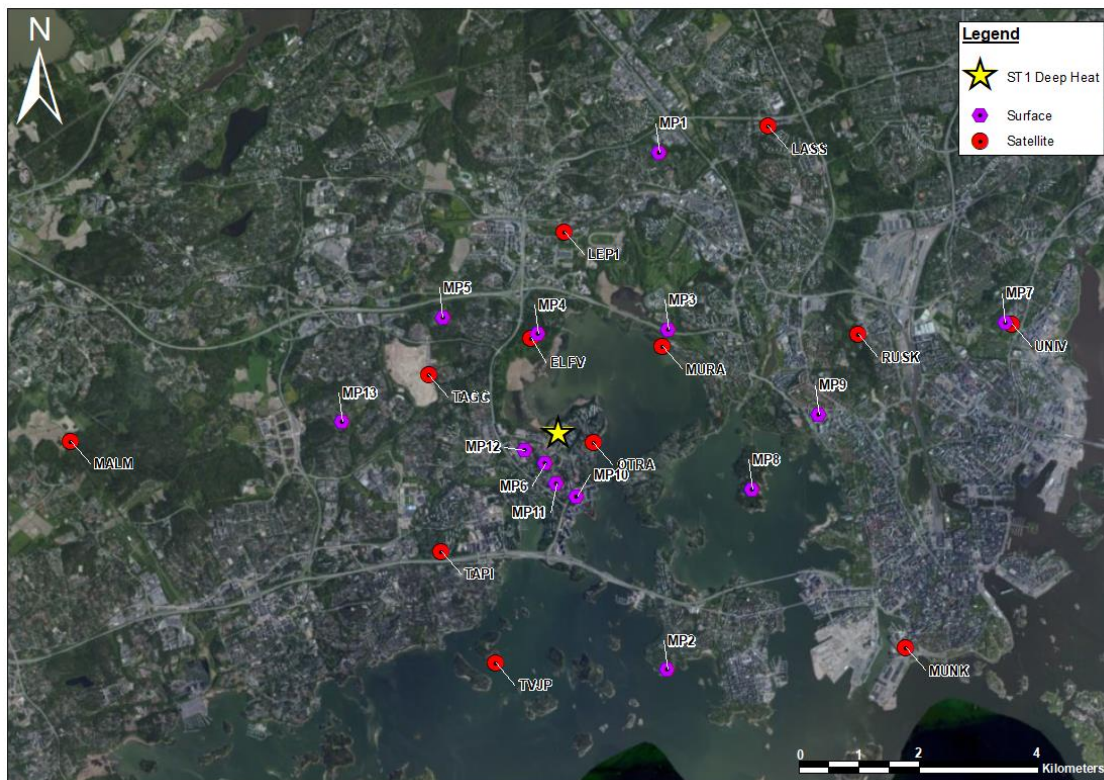


Figure 2: Location Map of the Monitoring Networks used for the TLS

TLS Design and Approval Strategy

Methodology

The TLS to be designed aimed at reducing the induced-seismicity hazard in order to regulate and mitigate the risk of adverse public response and the risk to the built environment. The challenges specific to this specific TLS design were the following:

- Owing to the low levels of seismicity in Finland, there was very little seismic data available for the calibration and design of the TLS;
- The stimulation took place in a large urban area, which meant a large and densely populated area with multiple sensitive receptors and high levels of vibration noise (especially from construction blasting), which posed a risk of false alerts; and
- The population was reportedly very sensitive to earthquakes, bearing the risk of bad public perception, which has been known to shut off geothermal projects in the past (e.g., Giardini, 2009; Diehl et al., 2017).

The strategy to build the TLS was therefore based on thresholds related to acceptable ground motion levels, on one hand, and on probabilities to reach these thresholds, on the other hand. From the point of view of having the TLS approved by a regulator, basing it on acceptable levels of ground motion facilitated the discussions. A consensus is easier to reach on ground motions than on event magnitudes, as discussion rely on factual arguments, such as existing regulations and best practices on ground vibrations.

For the stimulation of OTN-3, peak ground velocity (PGV) was selected as the measure of ground motion, as it is a simple parameter that has many engineering applications and it is regarded as a better indicator of the damage potential of the ground motion than peak ground acceleration (PGA) (Bommer, 2017).

Types of Thresholds

Basing a TLS only on PGV would potentially have had two issues:

- **False positives** (i.e., false alerts): High levels of PGV could be recorded that would not have been caused by induced earthquakes at the production site, but by blasting at the

surface, road traffic, equipment malfunction, distant natural earthquakes or other sources; and

- **False negatives** (i.e., no alert when there should be one): By nature, the PGV can only be measured at the specific locations where instruments have been installed. PGV thresholds could be exceeded at locations where no instrument was recording and would therefore be missed.

To circumvent these issues, two types of thresholds were developed in parallel:

- **Joint PGV-magnitude alert:** When a PGV exceeding one of the TLS threshold was measured, a seismic event at the production site had to also be detected, which magnitude was large enough to trigger such a level of ground vibration. This process was aimed at reducing the risk of false alerts; and
- **Magnitude-only alerts:** If an earthquake was detected during operations, which had the potential to generate a PGV exceeding one of the PGV thresholds, an alert would be triggered, even if no PGV was measured at any of the surface geophones above the TLS thresholds. This type of alert was aimed at reducing the risk of missed alerts.

Therefore, PGV thresholds had to be completed with associated event magnitudes, which was done through various ground motion prediction equations (GMPE). The process is described in detail later.

PGV Thresholds

General PGV thresholds were developed in accordance with Finnish Building Code, British Standards on surface vibrations and various publications illustrating the relationship between PGV and impacts on human perception and the built environment (e.g., Westaway *et al.*, 2014; Bommer, 2017). Figure 3 illustrates some of the relationships between PGV and impacts on the surrounding environment, as developed by Bommer (2017) and proposed in the British Standards (BS 7385-2:1993, BS 6472-1:2008).

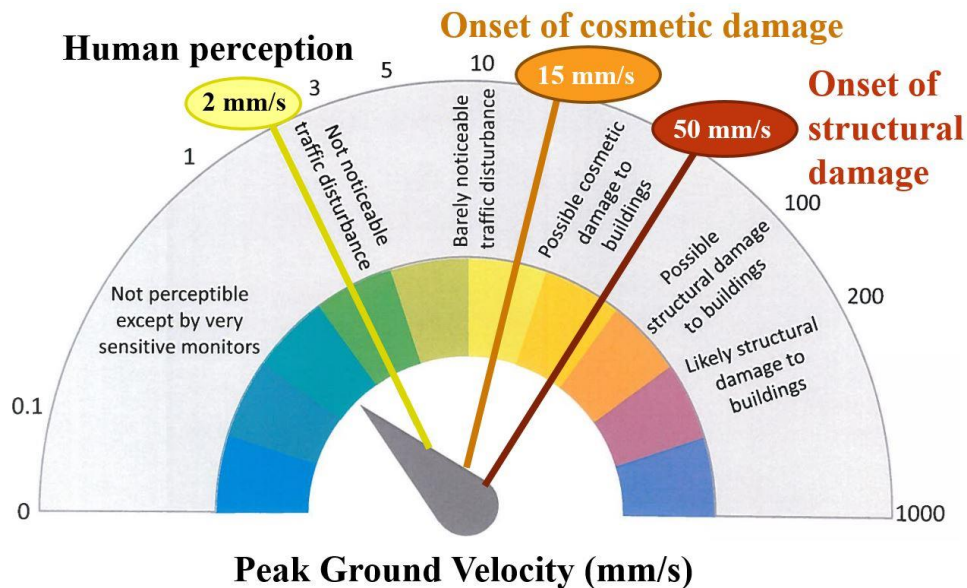


Figure 3: Relationship between PGV and impact (adapted from Bommer, 2017; BS 7385-2:1993 and BS 6472-1:2008)

Table 1 summarises some typical PGV thresholds not to be exceeded according to vibration requirements of a construction site on a variety of soil types for a range of structures and materials, as described in the Finnish Building Code: Vibrations caused by construction (RIL 253-2010).

An important distinction to note is the difference between seismic waves from deep geothermal injection and source of vibrations during construction related blasting. During construction related blasting, the propagation of waves is predominantly horizontal from sources at the surface. In contrast, the propagation of seismic waves from a deep geothermal activity (in this case over 6

km deep) is largely vertical. Thus, the Finnish Building Code guidance provided in Table 1 should be considered in context of this difference. Due to the different nature of the seismic propagation, only the PGVs for nearby blasting events are considered relevant. In addition, while there certainly exists many areas throughout Helsinki and Espoo where clays and other soils exist, these soils are still relatively shallow from the context of vertical seismic wave propagation. Therefore, only materials with $V_P \geq 2,000$ m/s were considered relevant to compare PGV thresholds.

Soil Type	Soft Clay	Resilient Clay, Silt, Sand	Moraine, Gravel, Compact Sand	Hard Rock
P wave velocity (V_P) for Surface Blasting	< 1,000 m/s	1,000 – 1,500 m/s	2,000 – 3,000 m/s	> 4,000 m/s
Bridges, Docks, etc.	15.75 mm/s	31.5 mm/s	61.25 mm/s	245 mm/s
Concrete and Steel Industrial	11.25 mm/s	22.5 mm/s	43.75 mm/s	175 mm/s
Concrete and Steel Housing	9 mm/s	18 mm/s	35 mm/s	140 mm/s
Brick Buildings	7.65 mm/s	15.3 mm/s	29.75 mm/s	119 mm/s
Light Weight Brick Buildings, Churches, etc.	4.95 mm/s	9.9 mm/s	19.25 mm/s	77 mm/s
Note: Soft clay and resilient clay, silt, and sand are not relevant to the project site and are only provided for reference. The majority of the areas relevant to stimulation activities are related to hard rock.				

Table 1: Summary of Finnish Building Code for Surface Blasting Activities and Typical PGV Thresholds for Selected Structures and Materials on a Variety of Soil Types (RIL 253-2010).

The general PGVs selected were developed for **Green**, **Amber** and **Red** conditions, based on Figure 3, with sufficient factors of safety added, as indicated below. The selected thresholds were also conservative with respect to values indicated in Table 1. The selected PGV thresholds were as follows:

- **Green** conditions: **PGV = 0.3 mm/s**. This low level was set in surface network stations to generate low level alarms in the form of text messages to a dedicated site phone. This low-level condition provided sufficient feedback that surface network stations remained operational. This threshold was selected as it was well below the threshold of human perception indicated in Figure 3;
- **Amber** conditions: **PGV = 1 mm/s**. This level correlated with the lower threshold of human perception indicated in Figure 3, with a factor of safety of two. While a PGV of 1 mm/s might, in some rare cases, be noticed by the local community, no credible impacts would be expected; and
- **Red** conditions: **PGV = 7.5 mm/s**. This level correlated with the lower threshold of potential cosmetic damage indicated in Figure 3 with an additional factor of safety of two. This threshold was considered conservatively reasonable since stimulation activities would be halted prior to any cosmetic or other (i.e. structural) impacts.

Sensitive Receptors

A survey of local receptors was performed by the St1 DH team, who identified six sensitive receptors. One surface station was placed at each of these sensitive receptors in order to specifically monitor ground motions at these locations: surface stations MP6, MP7 and MP9 to MP12 were each specifically dedicated to a sensitive receptor (Figure 2).

Specific TLS ground motion thresholds were investigated independently for each of the sensitive receptors. Depending on the receptors, the ground motion requirements were either defined in terms of PGV or PGA.

It turned out that, for four of the six sensitive receptors, the general TLS PGV thresholds were more conservative than the requirement of the specific sites. The general TLS thresholds were therefore selected at these sites.

The last two receptors had requirements in terms of PGA and specific thresholds were established at the levels of **PGA = 1%g** for the **Amber** threshold and **PGA = 7.5%g** for the **Red** threshold.

Magnitude Thresholds

As discussed earlier, the PGA and PGV thresholds for the TLS were related to event magnitudes through the use of different GMPEs.

GMPE in PGA

ISUH provided a GMPE in PGA, based on PGAs measured in Finland for events between magnitudes of -0.9 and 4.1 and hypocentral distances ranging from 1.5 to 78 km. The magnitude scale used by ISUH was the local 'Helsinki' magnitude, M_{L_HEL} (Uski and Tuppurainen, 1996).

A comparison of the predictions of the ISUH GMPE to other GMPEs published in the geothermal context (Douglas, 2013) indicated that the GMPE provided by ISUH predicted higher levels of PGA at all magnitudes. It was therefore deemed suitable for use in the TLS, as it was unlikely to yield under-conservative estimates.

GMPEs in PGV

No GMPE was available from ISUH in terms of PGV. PGV data was provided by ISUH for the same events used to determine the GMPE in terms of PGA, but a review of these PGV values concluded that they were unrealistically low and were therefore deemed inappropriate to develop a specific PGV GMPE for use in the TLS.

To circumvent the absence of local GMPE in PGV for the TLS, two options were followed:

- Use the general GMPE in PGV by Douglas (2013); and
- Adapt the GMPE in PGA by ISUH (2017).

The GMPE by Douglas (2013) was relevant to the project, as it was developed specifically for geothermal activities for hard-rock sites. Douglas (2013) took data from several geothermal sites across the world, adjusted them for hard-rock conditions and deduced a global GMPE. The uncertainties on this GMPE are large, as they capture the variability from one site to the other. This GMPE was therefore deemed suitable for this project. The magnitude scale used in the GMPEs by Douglas (2013) was the moment magnitude M_w , which was related to the local 'Helsinki' magnitude using the relationship published by Saari et al. (2015):

$$M_w = 0.8M_{L_HEL} + 0.33. \quad (1)$$

In order to adapt the GMPE in PGA by ISUH (2017) to PGV, we used the observation that published GMPEs for geothermal areas displayed large similarities between PGA and PGV. Douglas (2013) simply had:

$$\ln PGV (mm/s) = \ln PGA (\%g) + 0.5. \quad (2)$$

Similarly, Sharma (2013) wrote:

$$\ln PGV (mm/s) = \ln PGA (\%g) - 0.3 + 0.1 * M_w, \quad (3)$$

We therefore used the GMPE by ISUH in terms of PGA as a proxy for the GMPE in terms of PGV:

$$\ln PGV (mm/s) = \ln PGA (\%g). \quad (4)$$

Using such a proxy added uncertainty to the median predictions, which was accounted for by adding a factor of 0.5 to the standard deviation of the $\ln PGA$ of the GMPE by ISUH. The value of 0.5 was based on Equations (2) and (3), and considering that, in Equation (3), the magnitude of events induced and in use for the TLS would fall well within the range of $-1 \leq M_w \leq 4$.

Probability of PGV Exceedance

For simplification, equations and explanations are expressed in terms of PGV in this section, but the logic remains the same for PGA.

The GMPEs presented in the previous sections were used to determine reasonable magnitudes associated to the different PGV thresholds. These magnitudes were obtained by first agreeing with the regulator what “reasonable” would mean in terms of probabilities to exceed a PGV threshold. Specifically, two probabilities needed to be agreed upon, for the two types of alerts in use in the TLS:

- **Joint PGV-magnitude alert:** When a PGV exceeding one of the TLS thresholds would be measured and an induced event detected, what would be the probability below which the event magnitude would be considered too small and could not be responsible for such a PGV exceedance?
- **Magnitude-only alerts:** If an earthquake were detected during operations but no PGV exceedance were measured, what would be the probability above which the event magnitude would still be considered large enough to have potentially generated a PGV exceedance?

The two following probabilities were therefore agreed for the two types of thresholds considered for the **Amber** alert:

- Magnitudes associated to joint PGV-magnitude alerts were selected based on a 2% probability that the seismic event would cause a PGV exceedance; and
- Magnitudes associated to magnitude-only alerts were selected based on a 10% probability that the magnitude would result in a PGV exceedance.

In order to simplify the **Red** trigger of the TLS, it was agreed that a TLS alert would be conservatively triggered by the occurrence of a seismic event with only 2% probability to cause a **Red** PGV exceedance at the epicentre.

Magnitude Thresholds

The probabilities of exceedance of the different PGV thresholds were computed as a function of the different magnitudes and then used to inform the magnitude thresholds.

All GMPEs used in this study followed a lognormal distribution, i.e., the natural logarithm of the PGV predicted by the GMPE followed a normal distribution, with mean value $\ln PGV$ and standard deviation σ .

The probability of exceedance of a PGV threshold was therefore simply expressed as:

$$P_{exc}(th) = \frac{1}{2} \left[1 - \operatorname{erf} \left(\frac{\ln th - \ln PGV}{\sqrt{2}\sigma} \right) \right], \tag{5}$$

where $\ln PGV$ and σ respectively are the mean and the standard deviation of the natural logarithm of the PGV predicted by the GMPE, $\ln th$ is the natural logarithm of the PGV threshold and $\operatorname{erf}(\cdot)$ denotes the classical error function:

$$\operatorname{erf}(x) = \frac{1}{\sqrt{\pi}} \int_{-x}^x e^{-t^2} dt. \tag{6}$$

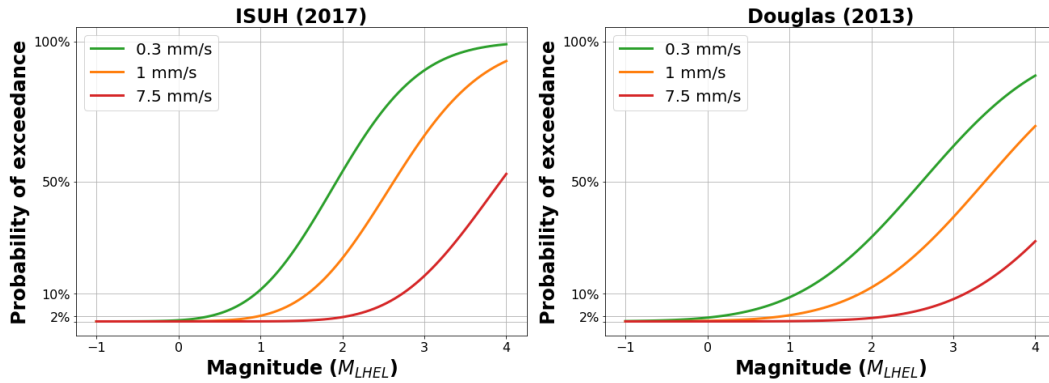


Figure 4: Probability of exceedance of different PGV thresholds for the two GMPEs used in this study.

Figure 4 shows the probability of exceedance of the three different PGV thresholds used in the TLS, for the two GMPEs in PGV selected in this study. These probabilities of exceedance were

calculated at the epicentre of earthquakes happening at 6 km depth, i.e., at hypocentral distances of 6 km.

Figure 5 shows the probability of exceedance of different PGA thresholds respectively for the GMPEs in PGA by ISUH (2017) and by Douglas (2013). Following the process for the PGV thresholds, these probabilities of exceedance were calculated at the epicentre of earthquakes happening at 6 km depth. The PGA thresholds in Figure 5 correspond to the PGA thresholds considered for the TLS.

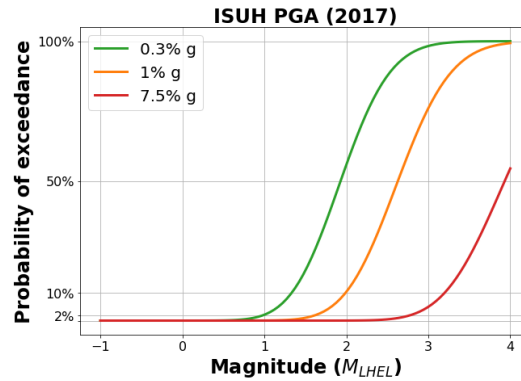


Figure 5: Probability of exceedance of different PGA thresholds for the GMPE in PGA by ISUH used in this study.

The magnitudes corresponding to the 2% and 10% probability of exceedance of the PGV thresholds, which can be read on Figure 4, are detailed in Table 2 and Table 3.

	2% exceedance probability		
	0.3 mm/s	1 mm/s	7.5 mm/s
ISUH PGA (2017)	0.4	1	2.1
Douglas (2013)	0.5	1.1	2.1

Table 2. Magnitudes that have a 2% probability to exceed the different PGV thresholds, for an event at 6km depth.

	10% exceedance probability		
	0.3 mm/s	1 mm/s	7.5 mm/s
ISUH PGA (2017)	0.9	1.6	2.7
Douglas (2013)	1.2	1.8	2.8

Table 3. Magnitudes that have a 10% probability to exceed the different PGV thresholds, for an event at 6km depth.

Table 2 and Table 3 show that the magnitudes obtained with the GMPE in PGV by Douglas (2013) and by the proxy with ISUH PGA (2017) were quite similar, both for the 2% and 10% exceedance probabilities. This increased the level of confidence in using these two GMPEs for PGV with their respective uncertainties.

From Table 2, it was agreed that an event with $M_{L_HEL} \geq 2.1$ would trigger a **Red** event, while any $PGV \geq 7.5$ mm/s would need to be reported.

For the **Amber** alert, it was also agreed from Table 2 that if a PGV at any of the stations exceeded 1 mm/s during an event, if that event had $M_{L_HEL} \geq 1.0$, then an **Amber** alert would be triggered (joint PGV-magnitude alert).

Table 3 indicates that if no $PGV \geq 1$ mm/s was measured at any of the surface stations, an **Amber** alert should still be triggered if a $M_{L_HEL} \geq 1.6$ event was detected (magnitude-only alert). However, in this case, the regulator judged that the threshold was too high and requested that it be lowered to 1.2. Even though the value of 1.2 was deemed too conservative, it was finally agreed that the magnitude-only **Amber** alert would be triggered for $M_{L_HEL} \geq 1.2$.

Equivalently, the magnitudes corresponding to the 2% and 10% probability of exceedance of the PGA thresholds, which can be read on Figure 5, are detailed in Table 4. As was done for the

PGV, Table 4 was then used to associate magnitudes to PGA thresholds at the sensitive receptors.

	ISUH PGA GMPE (2017)		
	0.3% g	1% g	7.5% g
2% exceedance probability	1	1.6	2.8
10% exceedance probability	1.3	2	3.2

Table 4. Magnitudes that have a 2% and 10% probability to exceed the different PGA thresholds, for an event at 6km depth, according to the GMPE by ISUH (2017).

Conclusion

The TLS designed for the stimulation of the geothermal well OTN-3 in the Helsinki area was based on two main parameters:

- The acceptable levels of ground motion caused by induced events; and
- The probability to reach these levels.

From this basis, two types of TLS alerts were developed, in order to minimize the risk of false alerts or missed alerts:

- One threshold based on ground-motion threshold exceedance confirmed by a seismic event of tangible magnitude; and
- One threshold based on event magnitude only.

In order to simplify the TLS, the Red trigger was reduced to the magnitude-only trigger. The final TLS used during the stimulation of OTN-3 is summarised in Figure 6.

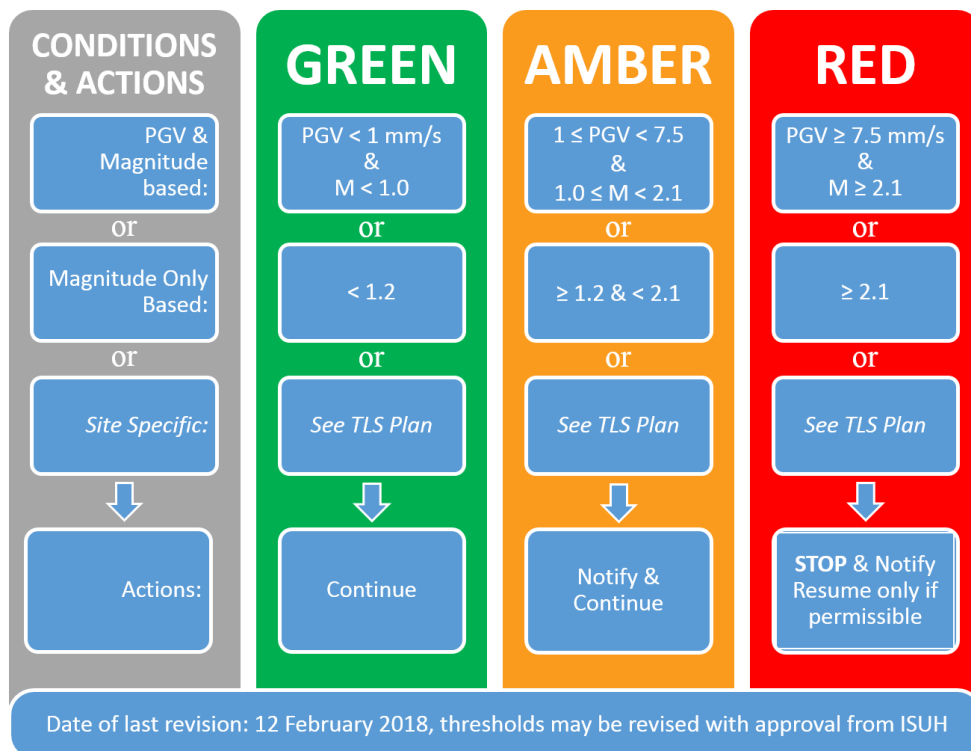


Figure 6: Summary of TLS for St1 Deep Heat.

Specific receptors were also identified for the project and each of them was equipped with a surface station, to specifically monitor vibrations related to induced seismicity at these locations. Specific thresholds were put in place at these receptors, which were integrated into the more general TLS.

Seismic monitoring networks were put in place, with sufficient redundancy to confidently detect seismic events, compute their source parameters in near-real time, and monitor the surface vibrations originating from these induced events. The stimulation proceeded guided by the TLS

limits, with the observed seismicity used to limit stimulation, thereby avoiding a project-stopping event.

References

- Bommer, J. J. (2017). Predicting and Monitoring Ground Motions Induced by Hydraulic Fracturing, OGA-commissioned paper.
- BS 7385-2:1993. Evaluation and measurements for vibration in buildings – Part 2: Guide to damage levels due to groundborne vibration. British Standards Institute.
- BS 6472-1:2008. Guide to evaluation of human response to vibration in buildings – Part 1: Vibration sources other than blasting. British Standards Institute.
- Diehl, T., Kraft, T., Kissling, E. and Wiemer, S. (2017). The induced earthquake sequence related to the St. Gallen deep geothermal project (Switzerland): Fault reactivation and fluid interactions imaged by microseismicity. *Journal of Geophysical Research: Solid Earth*, doi:10.1002/2017 JB014473.
- Douglas, J., Edwards, B., Convertito, V., Sharma, N., Tramelli, A., Kraaijpoel, D., Cabrera, B.M., Maercklin, N., Troise, C., (2013). Predicting ground motion from induced earthquakes in geothermal areas. *Bulletin of the Seismological Society of America*, Vol. 103, 1875–1897.
- Giardini D (2009). Geothermal quake risks must be faced. *Nature*. 462: 848-849.
- Kwiatek, G., Saarni T., Ader, T., Bluemle, F., Bohnhoff, M., Chendorain, M., Dresen, G., Heikkinen, P., Kukkonen, I., Leary, P., Leonhardt, M., Malin, P., Martínez-Garzón, P., Passmore, K., Passmore, P., Valenzuela, S., Wollin, C. (2019, in press). Controlling Fluid-Induced Seismicity during a 6.1-km-deep Geothermal Stimulation in Finland. In Press, *Science Advances*, March 2019.
- RIL 253-2010. Rakentamisen aiheuttamat tärinät 2010. Helsinki: Suomen Rakennusinsinöörien Liitto
- Saari J, (ed.), Lund B, Malm MM, Mäntyniemi PB, Oinonen KJ, Tiira T et al. (2015). Evaluating Seismic Hazard for the Hanhikivi Nuclear Power Plant Site, Seismological Characteristics of the Source Areas, Attenuation of Seismic Signal, and Probabilistic Analysis of Seismic Hazard. ÅF-Consult Ltd, 258 p.
- Sharma, N., Convertito, V., Maercklin, N., Zollo, A. (2013). Ground-Motion Prediction Equations for The Geysers Geothermal Area based on Induced Seismicity Records. *Bulletin of the Seismological Society of America*, Vol. 103, No. 1, pp. 117–130, doi: 10.1785/0120120138.
- Uski, M. and Tuppurainen, A. (1996). A new local magnitude scale for the Finnish seismic network. *Tectonophysics*, Volume 261, Issues 1–3, 23–37, [https://doi.org/10.1016/0040-1951\(96\)00054-6](https://doi.org/10.1016/0040-1951(96)00054-6).
- Westaway, R. and Younger, P. L. (2014). Quantification of potential macroseismic effects of the induced seismicity that might result from hydraulic fracturing for shale gas exploitation in the UK. *Quarterly Journal of Engineering Geology and Hydrogeology*, 47(4): 333–350. doi: <https://doi.org/10.1144/qjegh2014-011>